IEEE Access
Multidisciplinary | Rapid Review | Open Access Journal

Received April 23, 2018, accepted June 3, 2018, date of publication June 14, 2018, date of current version July 19, 2018.

Digital Object Identifier 10.1109/ACCESS.2018.2847314

Falcon: Fused Application of Light Based Positioning Coupled With Onboard Network Localization

DANIEL KONINGS[1], (Member, IEEE), BADEN PARR[1], FAKHRUL ALAM[1], (Member, IEEE), EDMUND M.-K. LAI[2], (Senior Member, IEEE)

[1]School of Engineering and Advanced Technology, Massey University, Auckland 0632, New Zealand
[2]Department of Information Technology and Software Engineering, Auckland University of Technology, Auckland 1142, New Zealand

Corresponding author: Daniel Konings (d.konings@massey.ac.nz)

This work was supported in part by the Massey University Research Fund (MURF) and in part by Rexel Lighting.

ABSTRACT Indoor localization based on visible light and visible light communication has become a viable alternative to radio frequency wireless-based techniques. Modern visible light position (VLP) systems have been able to attain sub-decimeter level accuracy within standard room environments. However, a major limitation is their reliance on line-of-sight visibility between the tracked object and the lighting infrastructure. This paper introduces fused application of light-based positioning coupled with onboard network localization (Falcon), a VLP system, which incorporates convolutional neural network-based wireless localization to remove this limitation. This system has been tested in real-life scenarios that cause traditional VLP systems to lose accuracy. In a hallway with luminaires along one axis, the Falcon managed to attain position estimates with a mean error of 0.09 m. In a large room where only a few luminaires were visible or the receiver was completely occluded, the mean error was 0.12 m. With the luminaires switched off, the Falcon managed to correctly classify the target 99.59% of the time to within a 0.9-m^2 cell and with 100% accuracy within a1.6-m^2 cell in the room and hallway, respectively.

INDEX TERMS Indoor positioning systems (IPS), indoor localization, visible light communication (VLC), visible light positioning (VLP), zigbee localization, convolutional neural network (CNN).

I. INTRODUCTION

Indoor localization techniques could be classified into two categories: Device-Free Passive (DFP) and Active Tracking [1]. In DFP systems, the tracked target does not actively contribute to the localization effort. This allows these systems to provide generic services like intruder detection or automated lighting schemes based on human presence. Active Tracking systems are ones that require the tracked entity contributes to the localization effort. These systems benefit from knowing the identity of each tracked entity, enabling them to provide targeted services like individualized advertising, patient monitoring and asset tracking.

Most indoor localization implementations require sensors to be embedded within the target environment at regular intervals to ensure the localization error is minimized across the whole area of interest. For this reason, initial implementation costs for existing buildings can be high. In this paper a system that utilizes the existing infrastructure to provide indoor localization as a secondary service is proposed. It is based on an Active Tracking approach and incorporates fusion between visible light positioning (VLP) and radio frequency (RF) wireless localization.

In a preexisting built environment, the position of light sources or luminaires is dictated by the need for adequate illumination as per indoor lighting standards, e.g. AS/NZS-1680 [2]. The position of the luminaires may not be optimum from the perspective of localization. For smart lights, there is often a Wi-Fi/Zigbee radio incorporated as part of the light to allow for the light to be controlled through a network. We overcome the inaccuracies resulting from non-ideal placement of smart lights by combining location information from both luminaire and wireless sources. Visible Light Positioning (VLP) systems rely on the target to maintain Line-Of-Sight (LOS) with the luminaires mounted within the environment. This means that VLP approaches suffer from blind spots when the target does not maintain LOS with an adequate number of luminaires, e.g. when the target passes under a table. Another problem arises in hallways which are

2169-3536 © 2018 IEEE. Translations and content mining are permitted for academic research only.
Personal use is also permitted, but republication/redistribution requires IEEE permission.
See http://www.ieee.org/publications_standards/publications/rights/index.html for more information.

typically illuminated by a single row of lighting sources. This causes issues with traditional VLP trilateration techniques as the system only has access to position information along a single axis. Since wireless signal experiences complex multipath propagation, wireless transceivers can contribute to horizontal awareness even when arranged in a single row. VLP systems also require the luminaires to be switched on which limits their use in many situations. This can be rectified by wireless augmentation. The fusion of two techniques for localization also makes the system robust, provides redundancy and fault tolerance.

The proposed solution uses slightly modified commercial luminaires and a collocated ZigBee radio to represent commercial smart lights, a photo diode coupled with a ZigBee radio as a target entity and a computer to collect all information and infer a targets location.

We propose a VLP implementation using carrier frequency allocation by inserting small amplitude sinewaves [3] biased close to the nominal voltage of the luminaire driver to provide unique ID for each luminaire. The implementation is similar to Intensity Modulation / Direct Detection (IM/DD) [4] with the difference being there is no data on the carrier. Since the lights are primarily utilized for illumination, On Off Keying (OOK) with 100% modulation depth [5] is not suitable for a VLP system using an existing lighting infrastructure since it causes a significant reduction in transmitted power resulting in lower brightness. Another major concern is that OOK creates harmonics which require more complicated multiplexing and reduce its scalability.

II. RELATED WORKS

In recent years indoor localization has been a popular research topic, partially due to the accuracy limitation of GPS signals within indoor environments. If accurate indoor localization schemes could be developed there would be many potential uses including smart robotics, elderly healthcare, targeted marketing, search and rescue etc. Wireless methods include RFID [6], ZigBee [7]–[9], Wi-Fi [10], [11] and Bluetooth [12], [13]. A common problem with traditional wireless approaches is that they suffer from multipath degradation [14], [15], interference [16] and struggle to attain a sub meter resolution. Some recent approaches have used visible light communication (VLC) for visible light positioning (VLP). Current methods either use a camera to take decodable images of the luminaires [17], or utilize a photodiode ranging methodology [18].

A. RF LOCALIZATION

Range-based localization methods attempt to create a functional model that accurately describes the relationship between received signal strength and distance, i.e. the path-loss regression model. After this model has been established, there are several methods for locating a remote Radio Frequency (RF) entity.

Lateration approaches require the tracked RF entity to be in contact with at least 3 known anchor nodes. Once this requirement is met, they use a least squares method to derive the entity's location [19]. These types of method can work well in open spaces, but often struggle to attain acceptable accuracy in indoor environments as they do not properly account for multipath propagation. Attempts have been made to enhance the accuracy of RF based lateration approaches by dynamically changing the propagation model in real time [20], but the systems are still unable to attain sub meter level accuracy.

The Maximum Likelihood Estimation (MLE) approach to localization works by treating the distance between known nodes and unknown nodes as an unknown random variable with Gaussian distribution [21]. The algorithm then finds the location of maximum probability, by minimizing the variance of estimated error. This approach is more accurate than traditional ranged approaches, but its performance is determined by the number of static nodes, and the assumption that the channel model for each TX-RX pair is independent.

RSSI Map approaches, also known as RSSI fingerprinting, [10], [22], [23] are implemented in a two-stage approach, offline training and online estimation. During the offline training stage, RSSI signatures are collected with the tracked entity present in multiple known locations within the deployment region. These signatures are then stored in a database for later use. In the online estimation stage, the system tries to match current RSSI readings with a known location in the stored database. The closest match to the live values is used to infer the entity's current location.

In an Active tracking approach, where the target caries a radio [10], [22], [23], the RSSI signature is made up of a vector of RSSI values measured between known nodes and an RF emitter the tracked entity carries. Liu, Darabi et al classify RSSI Map based algorithms into five further categories: k-nearest neighbour (KNN) [9], [24], probabilistic methods [25], neural networks [26], [27], support vector machines (SVM) [28] and smallest M-vertex polygon (SMP) [29].

This paper implements a neural network approach for the RF section as it requires minimal pre-knowledge of the expected distribution and characteristics of the measured RSSI data.

One of the major applications of the developed system could be asset tracking within built environment (e.g. tracking beds and medical equipment in a hospital). Therefore it is very important that the roaming target nodes are low cost, have long battery life, and do not interfere with existing infrastructure. Zigbee was chosen as the wireless resource as it is more energy efficient than Wi-Fi [30]. Zigbee networks also have been shown to have little impact on the throughput of neighboring Wi-Fi networks [31], [32], which means our implementation would not adversely affect existing wireless infrastructure. Finally, though Wi-Fi networks can impact the throughput of Zigbee networks, they do not affect the RSSI values of correctly received packets which are required for localization [16].

Channel State Information (CSI) has been shown to be a better metric for implementing indoor localization systems

than RSSI as it can mitigate the effects of multipath propagation [33], [34] resulting in higher accuracy. However, the CSI metric is not commonly accessible in Off-The-Shelf wireless equipment, and current localization implementations are based around custom drivers for a very limited set of Intel [35] or Atheros [36] hardware. CSI has not been utilized in Falcon for this reason. However, it is advised that future implementations should use CSI over RSSI if the metric receives widespread commercial adoption.

Even though RSSI localization is limited due to multipath-channel effects and RF interference, it can still provide coarse indoor localization estimates [7], [12], [37]. The role of RF localization in Falcons sensor fusion is to help mitigate the limitations of the more accurate VLP implementation.

B. VISIBLE LIGHT POSITIONING

Visible Light Positioning systems benefit from very dominant line-of-sight (LOS) components which help mitigate the effect of multipath which allows implementations to attain a higher accuracy than traditional RF based systems [38], [39]. Recent research into VLP largely falls into two approaches; photodiode-based localization or image-sensor based localization. Photodiode approaches typically aim to triangulate/trilaterate a receiver node with reference to multiple stationary luminaires. This is accomplished by transforming chosen metric readings into an angle/distance from a specific luminaire. Some common metrics available to photodiode based VLP systems include received signal strength (RSS) [5], [40], time of arrival (TOA) [41], time difference of arrival (TDOA) [42], [43] or angle of arrival (AOA) [44], [45]. When multiple luminaires are concurrently visible, a multiplexing scheme [3], [46] needs to be employed to ensure the receiver can decode and isolate the metric for each luminaire. For VLP approaches using phosphor-coated white LEDs, the accuracy is limited by the signal bandwidth since the response speed of the phosphor coating is slow. However, the bounds on position estimation accuracy are typically within the order of centimeters which is suitable for most indoor localization systems [41], [47].

Image-sensor based VLP uses a camera to capture an image of the visible luminaires. This approach benefits from less multi-luminaire interference than photodiode approaches as the image contains physically separated luminaires. A downside of this approach is that the off-the-shelf camera sensors may be required to exploit the rolling shutter effect to attain decodable images [38]. Since physical characteristics vary between camera sensors, image-sensor based VLP results may not translate between camera platforms. Another limitation is that the separation between the transmitter and receiver must be small to ensure each luminaire contains enough pixels within the image to localize [17]. Simulations involving typical indoor scenes, where the Cramer-Rao Lower Bound (CRLB) was derived show that the positioning accuracy of an Image-sensor approach is in the order of centimeters, with an azimuth angle error of less than 1 degree [47].

Recent VLP implementations include a novel Gaussian Process approach tracking a Tablet [48], with an average accuracy of 0.56m. However this work does not consider occlusion, as the receiver always maintain LOS with the luminaires. A hybrid solution was presented in [44] using simulated Wi-Fi and VLP with a reported accuracy of 0.1395m. However they did not implement a working system, and simulation also assumes ideal luminaires with no furniture within the room. Many implementations rely on a trilateration based approach [49] and recent implementations have been able to attain sub decimetre level accuracy within standard indoor environments [5], which is significantly better than the performance of most RF based RSSI implementations.

One of the major limitations of the reported physical implementations of VLP is that they do not properly account for the intermittent light occlusion that VLP receivers suffer from in common indoor, furniture rich environments. Our proposed system seeks to rectify the problem with occlusion by implementing a practical implementation featuring a fusion of a VLP receiver and zigbee radio. The fusion will also allow for localization in areas like hallways with row aligned VLP sensors that cannot normally converge and will allow for a coarse position estimate even when the luminaires are turned off. This will also provide localization results from multiple physical environments which is lacking in existing literature.

C. SENSOR FUSION

Multiple sensor approaches have been proposed for indoor localization in existing literature. Mobile phones are commonly used as localization targets which has allowed for the fusion of Inertial Measurement Unit (IMU), Wi-Fi and Bluetooth metrics for localization efforts [50]–[52]. Simultaneous Localization And Mapping (SLAM) was developed to help robots define their current location whilst also creating a map of the environment. SLAM implementations fuse information from multiple sensors to improve the accuracy of localization/mapping. Traditionally these systems have had a high implementation cost. However, recent research has looked into solving SLAM using low-cost sensors which typically fuse a camera with odometers and ultrasonic rangefinder sensors [53]–[55]. A comparison of the proposed Falcon and existing Sensor Fusion approaches is given in Table 1. As we can observe, the Falcon is very low cost, flexible and robust compared to the other existing systems.

D. CONTRIBUTION

As far as the authors are aware, this is the first reported work to physically implement a hybrid VLP/RF solution. The work also contains the following novel components:

1) The hybrid Falcon system (incorporating both VLP and RF) solves the problem of visible light occlusion within existing VLP approaches. This allows Falcon to work in realistic environments when the lights are not always turned on. Falcon also offers superior accuracy over

TABLE 1. Sensor fusion implementations.

Name	Technology	Average Accuracy	Tag Cost	Works in the dark	Resistant to Transient Interference	Works with Row Aligned Luminaires
Falcon	Photodiode RSS, Zigbee RSSI	0.12m	Low	Yes	Yes	Yes
KAILOS [57]	Wi-Fi RSSI, magnetometer, accelerometer, gyroscope, compass, barometer	1m	High	Yes	Unknown	N/A
LiFS [58]	Wi-Fi RSSI, accelerometer	5m	High	Yes	No	N/A
KILA [59]	Wi-Fi RSSI, RFID	>1m	Low	Yes	Yes	N/A
SVD-SF [60]	Image Sensor, accelerometer, gyroscope	0.05m	High	No	No	Unknown
LIPS [61]	Multiple Photodiode RSS, magnetometers, accelerometers	<1m	Medium	No	No	Unknown
Yasir et al [62]	Photodiode RSS, accelerometer	0.14m	Low	No	No	No
Yang et al [63]	Multiple Photodiode RSS, Multiple Photodiode AOA	0.06m	Low	No	No	Unknown

existing wireless approaches, when a lighting resource is available.

2) The proposed Falcon system presents a new hybrid Potential Fields and Neural Net based approach that has not previously been implemented for VLP or RF Indoor Localization.
3) Falcon is designed to work in hallways that feature row aligned luminaires, a scenario in which traditional VLP approaches are unable to converge.

III. SYSTEM OVERVIEW

The Falcon system tracks a target node based on its relative position to known ceiling mounted anchor nodes. The target node features a tag equipped with both a zigbee radio and a photodiode, whilst each anchor features a collocated VLP transmitter and zigbee module. VLP is the primary localization system in Falcon as it provides a higher accuracy than the wireless based localization. Wireless localization using zigbee is incorporated to overcome several key issues with the VLP localization approach. Firstly, it enables the system to remain operational when the lights are off. Secondly, it allows for localization even if the luminaires are mounted in a straight line or some of the luminaires are occluded. Finally, it prevents the VLP approach to converge to incorrect local minima.

The Falcon system works in two stages, as outlined in Fig. 1. During the Offline phase, the system collects both optical and RF samples. The RF samples are used to train a convolution neural net [56] that infers which region of interest (cell) a target is likely residing within. The optical samples are used to create two models. The first model maps the relationship between the received lights power intensity and the distance between the receiver and anchor nodes. The second model applies weights to the distance model based on how reliable the model is at varying distances from an anchor node.

The Online phase can be broken down into a further two stages. In the first stage, the RF neural net classifies a region of interest based on the trained model and the current RF samples. The system also uses the current optical samples to calculate a weighted distance between the tag and each anchor node. More details can be found in the Algorithm 1 pseudo-code. In the second stage, the iterative Force based Visible Light Positioning (FVLP) converges on a position estimate by using the RF region of interest as a starting point, and the VLP distances to refine a final estimate.

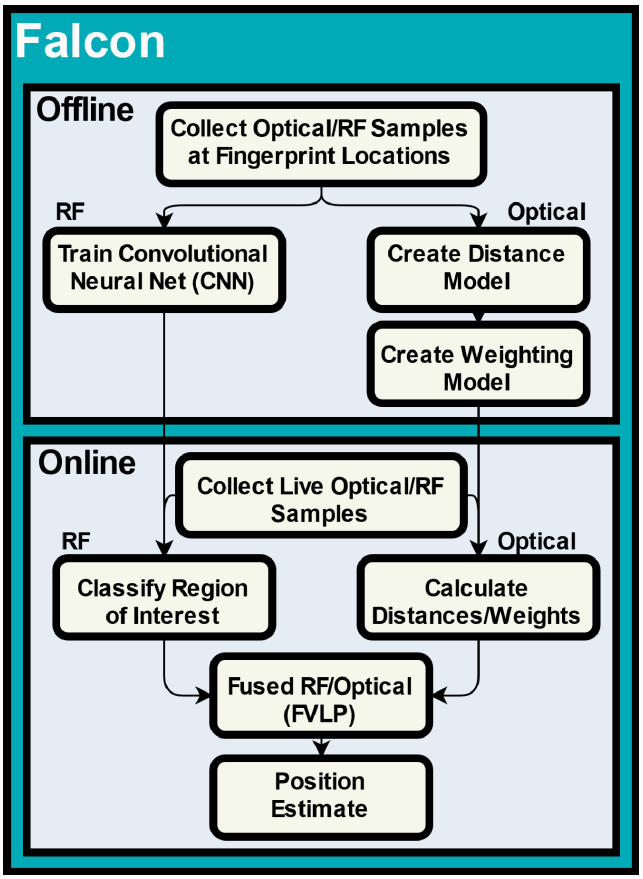

FIGURE 1. Falcon algorithm overview.

A. FALCON HARDWARE

The Falcon hardware was designed to use a remote tag node to receive optical and RF signals from ceiling mounted anchor nodes. The roaming target node periodically broadcasts a

communications request. Each ceiling node in range of this broadcast replies to the roaming node. The target records the RF RSSI value, ID and VLP power of each reply it receives and passes these to the processing computer for training during the offline period, or classification during the online phase. The Visible Light Positioning system consists of a photo diode acting as a receiver to measure the intensity of the received light at different frequencies. This approach was chosen over an image-sensor based approach as it allows for lower cost receivers (photodiode tags). One of the objectives of the developed VLP is to employ it for asset tracking by leveraging existing lighting infrastructure. Therefore a photodiode approach has deliberately been chosen as it makes the deployment of a large number of tags economically feasible. We also recognize the fact that phosphor-coated white LED luminaires are limited by their response time. However, off the shelf luminaires have been chosen to represent the realistic lighting infrastructure of a built environment. The developed VLP is not a VLC based data communication system. Rather than transmitting data, each luminaire is transmitting an unmodulated sinewave of a unique frequency so that the signal strength from each visible luminaire can be estimated. Therefore, the bandwidth constraint of the LEDs is not a major concern for our VLP approach. The bandwidth is large enough to accommodate a sufficient number of unique sinewave frequencies to be chosen to provide ID for each luminaire.

The photodiode intensity information is passed through an inverse Lambertian propagation model [64] to determine the distance between the receiver and each transmitter. A custom potential fields approach, FVLP, is then used to localize the target receiver.

Since this paper is focusing on systems that are affordable and could be implemented into preexisting built environments, a driver board was developed that can be retrofitted into existing LED luminaires by sitting between their driver and the luminaire itself.

The modulation/demodulation circuitry is based on IM/DD. The modulator was designed to work on frequencies between 2kHz and 4kHz. This allows the use of cheaper components as lower frequencies could be more easily generated and literature shows that any flicker generated above 1.25kHz can be considered low risk for humans [65]. The five frequencies chosen for modulation were 2.6kHz, 2.8kHz, 3kHz, 3.2kHz and 3.4kHz. A proportional integral system fine-tunes the oscillators. This results in a generated frequency error of less than 5Hz even with cheap capacitors and potentiometers.

The custom modulation boards were installed as part of the Anchor Nodes in two environments, a small Laboratory (1.8m $\times$ 2.7m) and an adjacent hallway shown in Fig. 2. A summary of the hardware used can be seen in Table 2.

FIGURE 2. Anchor nodes installed in hall.

TABLE 2. Falcon hardware.

Module	Name	Features
RF/VLP	Anchor Nodes	9 Ceiling Mounted CC2530 with ESP8266 and IM/DD modulator
RF/VLP	Tag Node	1 Mobile tag featuring a CC2530, ESP8266 equipped with a photo-diode
RF/VLP	PC	Win10 I7 Laptop with NVIDIA 960M Graphics Card and connected CC2530
VLP	Laboratory Luminaires	9 Ceiling Mounted REX13CDL

IV. Algorithm

As discussed before, Falcon requires an offline phase followed by an online one. During the Offline phase, Falcon is given a list of cell locations. Each cell represents an area of ground defined by user in advance. Further information about the cell layout used is given in Section V. Falcon takes the raw RSSI fingerprint values collected during the offline phase and allocates them to their appropriate known cell. These raw RSSI values, and their associated cell form the input data for training the CNN. During the Online phase, the trained CNN will then output (classify) a cell of interest, for any given raw RSSI input vector.

Falcon also creates a distance model between the tag and each of the anchor nodes using the VLP resources.

It should be noted that a CNN was chosen as it offers a simple implementation for classification based on raw RSSI values that have not been pre-processed, and where the absolute position of the anchor nodes may be unknown. Other approaches such as SVM, Particles Filters or Euclidean distance are also viable for providing a coarse RF based position estimate [66].

At the beginning of the Online phase, Falcon collects live RF and VLP samples. The RF section uses the live samples to infer a region of interest (cell) from the pre-trained CNN. The VLP section calculates the distances and weights from the live samples, based on the pre-calibrated models. The Potential Fields based VLP algorithm (FVLP) then uses the RF CNN cell of interest, VLP distances and VLP weights to iteratively converge on a final position estimate.

A. OFFLINE PHASE

During an initial calibration stage the target node collected optical samples in 13 locations in the Laboratory and Hallway respectively. RF samples were taken at 26 locations in the Laboratory and 18 locations in the Hallway. A raw RSSI sample is 1 byte long and represents a estimation of the received signal strength of a zigbee packet. The raw sample is converted to dBm by subtracting a vendor specific offset. A raw VLP sample is an estimation of the received power from the receiving photodiode. The output of the photodiode at location (x,y) is given by:

$$r(t) = \Sigma_{i=1}^{L} C_i B \sin(2\pi f_i t + \theta_i) \tag{1}$$

where L is the number of visible luminaires at location (x,y), B is the amplitude of the sinewave, f_i is the frequency of the sinewave ID of the i^{th} luminaire, θ_i is the phase of the sinewave ID of the i^{th} luminaire at location (x,y) and C_i depends on the response of the photodiode at the frequency f_i and the optical channel between the i^{th} luminaire and location (x,y). This is essentially a function of the distance, d_i between the photodiode at location (x,y) and the i^{th} luminaire.

By assuming that the receiver and transmitter planes are in parallel, we can simplify the well-known Lambertian propagation model [64] for the received power to:

$$P_{r,i} = \frac{P_t}{d_i^2}\left(\frac{m+1}{2\pi}\right) cos^m(\emptyset) A cos(\varphi) \tag{2}$$

where d_i is distance between the transmitter / receiver, m is the Lambertian order, $\emptyset$ is the irradiation angle, A is the area of the VLP detector, φ is the incidence angle, P_t is the power of the sinewave carrier and is given by $(B/\sqrt{2})^2$. This value is constant for all luminaires, at all receiver locations. $P_{r,i}$ is the received power of the i^{th} luminaires carrier.

Since the VLP transmitter and receiver planes are in parallel, we have $cos(\emptyset) = cos(\varphi) = h/d$. This allows for (2) to be further simplified to:

$$P_{r,i} = \frac{GP_t}{d_i^{(m+2+k)}} \tag{3}$$

where G is a constant gain of $A\left(\frac{m+1}{2\pi}\right)h^{(m+k)}$, and k is a constant added to adjust the fall off characteristics, which are affected by unique hardware differences in the transceiver pair.

Using the Pythagoras theorem, the radial distance is given by $d_{r,i} = \sqrt{d_i^2 - h^2}$. Combining this with (3) and rearranging, we have

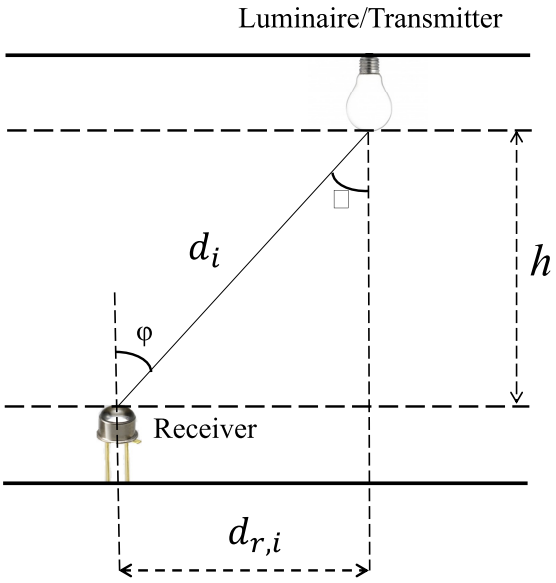

FIGURE 3. Side view of VLP system.

$$d_{r,i} = \sqrt{\left(\frac{GP_t}{P_{r,i}}\right)^{\frac{2}{(m+2+k)}} - h^2} \tag{4}$$

The relationship between the transmitting luminaire, the receiving photo-diode and the radial distance from (4) can be seen in Fig. 3. Since the environment contains multiple luminaires, we can estimate, $P_{r,i}$, the power for each luminaire by using periodogram analysis.

Assuming that $r(t)$ is windowed by a length-N window $w(n), 0 \le n \le N-1$, where $x(n) = r(t) \cdot w(n)$. The discrete-time Fourier transform (DTFT) of $x(n)$ is given by:

$$\mathrm{X}\left(e^{j\omega}\right) = \Sigma_{n=0}^{N-1} x(n) e^{-j\omega n} \tag{5}$$

This can be used to estimate the power spectrum as:

$$\hat{P}_{xx}(w) = \frac{1}{\beta N}\left|\mathrm{X}\left(e^{j\omega}\right)\right|^2 \tag{6}$$

where β is a constant normalization factor. We can ignore β as it will act as a constant scaling factor that would remain the same at all locations. We can use (6) and the known modulation frequencies to estimate the $P_{r,i}$ for each luminaire.

During the Offline phase, we collect $P_{r,i}$ estimates for each luminaire, at multiple locations (18 for the Hallway, 26 for the Laboratory) with known radial distances. We can then minimize the error between the estimated radial distances $(d_{r,i})$ and the actual radial distances $(d_{a,i})$ to attain the best values for G and k in (4). This can be defined as using minimization to solve :

$$\arg\min_{G,k} \left\| \boldsymbol{d_{r,i}} - \boldsymbol{d_{a,i}} \right\| \tag{7}$$

where $\boldsymbol{d_{r,i}}$ is a vector of the estimated radial distances from the i^{th} luminaires at the offline calibration locations

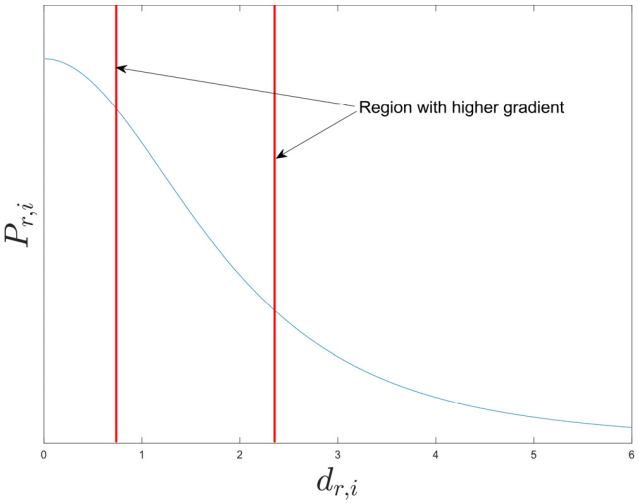

FIGURE 4. Model relating received power (Pr) and radial distance (dr).

(18 for the Hallway), and $\boldsymbol{d_{a,i}}$ is a vector of the actual corresponding radial distances.

Once optimal values are calculated for G and k, (4) can be used as a model to map a radial distance to any given luminaires P_r in the Online phase.

A typical model showing the relationship between $P_{r,i}$ and $d_{r,i}$ is shown in Fig. 4. The Lambertian model has regions with steep gradients, as shown in Fig. 4. Measurements from this region are preferable as $d_{r,i}$ has a higher resolution when predicted using equation (4). This can be exploited by weighting each luminaire with an absolute of the derivative of (8). This results in the region indicated in Fig. 4 receiving higher weights. The weighting index model ($W_{1:i}$) is created to act as an index lookup table which contains a weight model (W_i) for each luminaire within the system. When the system receives a new $P_{r,i}$ estimate, it is passed to the weighting index model which returns an individual weight. The process for creating each weight model (W_i) inside the weighting index model ($W_{1:i}$) is as follows. We rearrange (3) and (4) to obtain

$$P_{r,i} = \frac{GP_t}{(d_{r,i}^2 + h^2)^{\frac{m+2+k}{2}}} \tag{8}$$

Let

$$P_{r,i}^{'} = \left| \frac{d}{dd_{r,i}} P_{r,i} \right| \tag{9}$$

Then it can be normalized by

$$q_i = \left(\frac{P_{r,i}^{'} - \min(P_{r,i}^{'})}{\max\left(P_r^{'}, i\right) - \min(P_{r,i}^{'})} \right) \tag{10}$$

so that $0 \leq q_i \leq 1$. The i^{th} luminaires weighting model is then obtained by subtracting an LED's offset to shorten the tails, giving us

$$W_i = H(q_i - g_i) \tag{11}$$

where H is the Heaviside step function, used to set any tail with a negative weighting to 0, and g_i is the i^{th} luminaires tail offset.

Once the VLP distance model (4) and weight model (11) have been calculated, the system begins calibrating the wireless model. The wireless system uses the RSSI samples to create a convolutional neural network that divides the physical environment into predetermined grid sizes. The structure of the CNN used in Falcon is kept constant, but a separate CNN is trained for each partitioned location present. This has been done as it offers several benefits. Firstly, by having a smaller CNN that only incorporates the RF resources visible on a per location basis, CNN training is simplified. This means that on average it takes less than 2 minutes to train a room using the processing pc. RF localization systems based on RSSI are highly susceptible to multipath, which means their dynamics can significantly change due to environmental changes such as moved furniture. By segmenting the system per location, we can retrain the CNN on a per location basis. This ensures that the system is scalable and doesn't need complete retraining when environmental changes occur, but rather localized retraining should be sufficient.

A CNN was chosen as a fully connected architecture was deemed to be unnecessary for RSSI based localization as long as local features can be identified. Since RSSI data arrives at regular intervals at a higher frequency than expected movement, the data should exhibit strong autocorrelation over small intervals. Since convolutional networks assume locality, they should perform well with raw time series RSSI data.

When collecting offline samples, 800 samples were taken from each ceiling mounted radio within range, at each test point. In the hallway 5 radios were detected and measurements were taken at 18 test locations which resulted in a $[5 \times 800 \times 18]$ output RSSI array. To turn the RSSI samples into RSSI 'images' ready for CNN training, we create square matrices, grouping RSSI samples based on how many radios were detected. For the hallway scenario, this meant splitting each of the 18 test locations into 160 $[5 \times 5]$ matrices where each column represents RSSI from each radio and each row represents multiple samples from a single radio. These images are then randomly split in a 3 to 1 ratio of training images and validation images and passed to the CNN. The structure of the CNN used is outlined in Table 3.

The training was controlled by an output function which would stop the CNN training period if over any 6 consecutive validations, there had been no accuracy improvement seen in any of the validations. At this stage, the Falcon system transitions from the Offline training phase to the Online localization phase. A summary of the Offline phase is provided as Algorithm 1.

B. ONLINE PHASE – STAGE 1

The first stage of the Online phase involves preparing the inputs for the final iterative FVLP approach, as can be seen in Fig. 1. During each update, the RF section uses the live

TABLE 3. Convolution neural network parameters.

Layer	Name	Features
1	Image Input Layer	Hallway – 18 training points - 160 [5 x 5] samples Laboratory – 26 training points – 200 [4 x 4] samples
2	Convolutional Layer	16 3x3 filters, padding of 1
3	Batch Normalization Layer	
4	Activation Function Layer	ReLU
5	Convolutional Layer	32 3x3 filters, padding of 1
6	Batch Normalization Layer	
7	Activation Function Layer	ReLU
8	Fully Connected Layer	
9	Softmax Layer	
10	Classification Layer	

Algorithm 1 Offline Phase

procedure Calibration(*trainingLocations*, *LEDs*)
  Cells = number of cells
  $K[1 : count(LEDs)]$ = a constant per light derivative offset factor
  for each location in *trainingLocations* **do**
    $VLPfft = fft(location.signal)$
    $VLP\_Intensity = isolate\_per\_freq(VLP\_fft, LEDs)$
    if location is inside a new predefined cell **then**
      $Cell\_id = Cell\_id + 1$
    end if
    $RF\_data = [location.RF\_RSSI, Cell\_id]$
  end for
  $Distance\_vector = 0.01 : 0.01 : 8$ ▷ artificial distance index from 0.01 - 8m
  for $i = 1 : count(LEDs)$ **do** ▷ Calculate distance and weighting models for each LED
    $VLP[i].model = lambertian(VLP\_Intensity[i, :], LEDs[i])$
    $Power\_vector = inverse(VLP[i].model).predict(Distance\_vector)$
    $tempw = normalize(-1 * derivative(Power\_vector)) - K[i]$
    $VLP[i].weights = U(tempw) * tempw$ ▷ Where U(x) is the Unit Step Function
  end for
  $[RF\_t, RF\_v] = random(RF\_data)$▷ Randomly split into training/validation sets
  $RF\_CNN = train(RF\_t, RF\_v)$ ▷ Train the Neural Net
  Return $[VLP, RF\_CNN]$
end procedure

RSSI samples to classify a region of interest (cell) based on the pre-trained CNN from the offline phase. The VLP system estimates the received power from each luminaire and uses Equation (4) to map each received power measurement to a radial distance between the tag and its respective luminaire. Each luminaires distance is then assigned a weight by passing the distance through the weighting lookup table created during the Offline phase. Finally, the VLP Distances, VLP Weights and the CNN region of interest are passed onto the FVLP algorithm for final position estimation. Online Phase – Stage 1 is given by Algorithm 2.

Algorithm 2 Online Phase

procedure Localization(*VLP*, *RF_CNN*, *RF_RSSI*, *LEDs*)
  for each timestep **do**
    $VLP\_fft = fft(VLP.signal)$
    $VLP\_Intensity = isolate\_per\_freq(VLP\_fft)$
    $Cell = classify(RF\_CNN, RF\_RSSI)$ ▷ Retrieve the predicted cell from trained CNN
    for $i = 1 : count(LEDs)$ **do** ▷ Calculate radial distance and weight for each visible LED
      $VLP\_Distances[i] = VLP[i].model(VLP\_Intensity[i, :])$
      $weights[i] = VLP[i].weights(floor(VLP\_Distances[i]) + 1)$
    end for
    $Position = FVLP(LEDs, VLP\_Distances, weights, Cell)$
  end for
  Return *Position*
end procedure

C. ONLINE PHASE – STAGE 2

The FVLP system initializes its initial position state reported from the CNN as the center of the cell of interest. The FVLP localization system is an iterative approach that is based on the pathing method using Virtual Potential Fields [67], [68]. FVLP is passed a $d_{r,i}$ for each visible luminaire. This is equivalent to creating a circle around each luminaire with radius d_r as shown in Fig. 5. We define the distance between the previous position state and the current position state as:

$$\overrightarrow{d_{\Delta,i}} = P - L_i \tag{12}$$

where $\overrightarrow{d_{\Delta,i}}$ is the (x, y) distance vector between the previous position estimate and the ith Luminaire, P is the (x, y) coordinate of the previous position state estimate, and L_i is the (x, y) coordinate of the ith Luminaire.

If the previous position state lies outside the luminaire's circle, an attractive force is applied from the previous position state towards the luminaire's location. If the previous position state lies within the circle, a repulsive force is applied from the luminaires location towards the circles circumference. This is detailed in Fig. 9. The force applied to P, with respect to $L_i$can be defined as:

$$\overrightarrow{F_i} = -\left(\frac{\overrightarrow{d_{\Delta,i}}}{\left|\overrightarrow{d_{\Delta,i}}\right|}\right) F_{\mathrm{i}} \tag{13}$$

where F_{i} is defined as:

$$F_{\mathrm{i}} = S\left(\left|\overrightarrow{d_{\Delta,i}}\right| - d_{r,i}\right) W_i \tag{14}$$

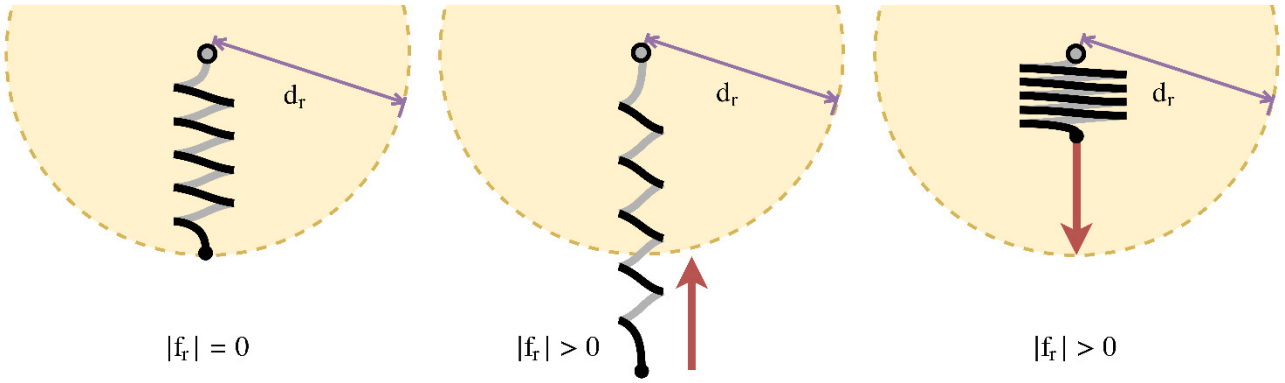

FIGURE 5. (a) FVLP force = 0. (b) Attractive force. (c) Repulsive force.

Algorithm 3 Visible Light Positioning - Force based Localization

```
procedure FVLP(LEDs, VLP_Distances, weights, RF_Cell)
    max_iterations = 100
    Position = center(RF_Cell)
    forceVector = [0, 0]
    stepSize = 0.1
    anchors.LEDs = LEDs
    anchors.weights = weights

    for i=1:max_iterations do
        netForce = [0, 0]
        for j=1:count(anchors) do
            deltaPos = Position − anchors(j).LEDs
            force = (mag(deltaPos) − VLP_
             Distances(j)) ∗ anchors(j).weights
            netForce = netForce − 1 ∗ (deltaPos/mag
            (deltaPos)) ∗ force
        end for
        Position = Position + netForce ∗ stepSize
        if mag(NetForce) < 0.01 then ▷ If convergence
        reached then return early
            break
        end if
    end for
    Return Position
end procedure
```

where S is a force scaling factor used to limit the maximum movement per iteration, $d_{r,i}$ is the radial distance of L_i, as defined in (4), and W_i is a weight for L_i, as defined in (11).

The total force applied at an iteration can be given by:

$$F_T = \sum_{i=1}^{L} \overrightarrow{F_i} \tag{15}$$

At the end of each iteration F_T is applied to P to attain a new position state estimate.

$$P_{new} = P + F_T \tag{16}$$

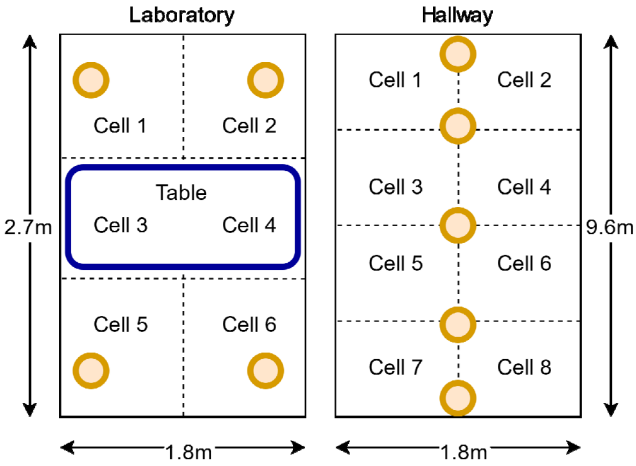

FIGURE 6. Laboratory and hallway cell layouts.

If F_T is very small or FVLP reaches its maximum allowable iterations, P_{new} is returned as the final position estimate. Otherwise P_{new} is used as P in the next iteration. The pseudo code for this process can be found in Algorithm 3.

V. EXPERIMENT AND RESULTS

The testing was undertaken in two locations (Laboratory room and Hallway) with two states (Smart Lights switched on /off). It is assumed that when a Smart Light is switched off, the luminaire is switched off but the radio resource remains available.

The laboratory area was split into 6 contiguous cells of 0.9m × 0.9m to define the test area. The Hallway was split into 8 contiguous cells with an average cell size of 0.9m × 2.4m. The test layouts can be seen in Fig. 6.

A summary of the Experimental Results can be found in Table 4.

A. EXPERIMENT 1 – LABORATORY – LIGHTS ON

In an ideal environment where the luminaries have good spatial separation across 2 axes, VLP localization can provide much higher accuracy than RF based active tracking.

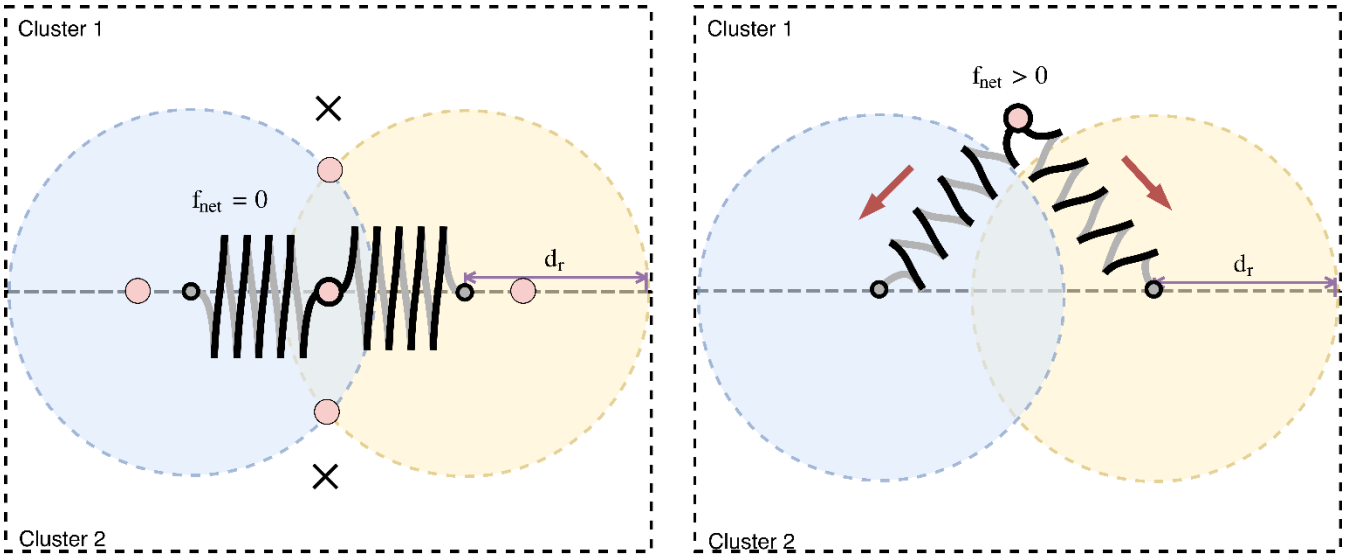

FIGURE 7. (a) FVLP Convergence issues. (b) FVLP forces direction.

TABLE 4. Experimental results.

Experiment	Accuracy	Max Error
Experiment 1	0.12 average error	0.4m when completely obscured by table
Experiment 2	99.59% cell classification	NA
Experiment 3	0.09 average error	0.16m
Experiment 4	100% cell classification	NA

The Falcon system uses the RF resource to define a region of interest. The region of interest is passed to the FVLP section which uses the VLP information to converge towards a refined position estimate.

The target traversed from one side of the room to another, passing under a table (where LOS to the luminaires was lost) in the process. The system was 100% accurate at detecting whether the target was underneath the table (and thus using RF tracking) or within an unobstructed area (using VLP). This translated to a real world error of less than 0.4m (cell level) when the lighting was completely occluded by the table. The system attained an average error of 0.12m for the rest of the room. It should be noted that the system was able to achieve a similar level of accuracy when partially occluded (only two luminaires visible when the tag is partially under the table) and when all luminaires were visible.

B. EXPERIMENT 2 – LABORATORY – LIGHTS OFF

When the lights are off the localization is estimated solely by the RF section. The CNN had a cell level accuracy of 99.92% during training. During the live period, the CNN was asked to classify live data based on the trained network. The target was positioned in 26 test locations within the laboratory, with 800 samples taken per location. The live samples were turned into RSSI 'images' in the same way as the training samples. The system could correctly classify which $0.9m^2$cell the target was in during the live phase with 99.59% accuracy.

C. EXPERIMENT 3 –HALLWAY – LIGHTS ON

In the hallway the luminaires are aligned in a single row. Traditional VLP will not function as trilateration schemes will not resolve due to the system only having information from one axis. It should be noted that VLP fingerprinting methods could also resolve this, but would require significant offline training to attain decimeter level accuracy.

To rectify this convergence issue, we first used the RF localization to determine a cell of interest. The center point of the chosen cell is then used as the initial position state estimate for the FVLP algorithm. As shown by Table 3, we were able to attain an average error of 0.09m, and a maximum error of 0.16m, as the system can correctly converge when initialized with a course localization estimate.

D. EXPERIMENT 3 –HALLWAY – LIGHTS OFF

During the live phase the target was randomly positioned 10 times with 800 samples taken per position. It was also ensured that at least one position was taken within each of the 8 cells. Both the trained CNN and live CNN classification had 100% accuracy. We attribute this localization improvement to the fact that the average cell size ($2.16m^2$) was larger than the laboratory ($0.9m^2$) and that the hallway was much less cluttered than the laboratory, reducing the effects of multipath.

E. RESULTS

F. CONVERGENCE

Typical trilateration schemes fail when the anchors are row aligned as there are multiple solutions. In Fig. 7a this can be

represented by the two red circles closest to the cluster centers which represent the two possible (mirrored) solutions.

The FVLP Potential Fields localization method has five possible locations of convergence as shown by all five red circles in Fig. 7a. FVLP has more regions of convergence than traditional trilateration because the dynamic weighting method used allows for the springs to have a net force of zero even if the current position estimate is not along the radial distances. The complete Falcon solution solves this by passing a cell center reference from the CNN implementation. The center of each cell (cluster) is represented by an 'X' in Fig. 7a. By passing the correct cluster center as an initial starting condition, the FVLP approach will converge towards the closest convergence candidate, which will always be the correct solution. This allows for the Falcon approach to correctly converge even if only two VLP anchors are visible. It also works when only one anchor is visible as the visible anchor will pull the coarse RF estimate towards a region of interest which will always offer higher accuracy than solely using the RF cell of interest.

Sensor fusion has been extensively studied in the literature and several common pitfalls have been identified [69]. In particular, the issue of poor performance due to incorrect sensor information is a valid concern. In Falcon we can identify 3 areas where performance may suffer; line of sight obstructions between the VLP receiver and ceiling mounted luminaries, multipath obstructions within the RF environment, and total loss of VLP information (e.g. the lights are switched off). Falcon has been implemented in a way that though these situations will cause performance degradation, the chance of critical failure is minimized.

The proposed FVLP approach has several features that facilitate its robustness. Namely, it runs in real time continuously during the online phase. It can identify sudden unexpected changes in VLP signal quality and react appropriately. In the case of complete VLP signal loss it can fall back to an RF based coarse position estimate.

If line of sight is lost between the VLP receiver and corresponding luminaire, sudden unexpected change in received power will result in a reduction of the weight/trust assigned to that link distance estimate. If two luminaries remain within sight of the receiver, the position estimate should not be affected. The trust/weight will be restored to the lost link when it reports a reasonable distance correlating with the remaining links. This means that performance is only reduced when only one luminaire is visible. The system's accuracy will still be higher than what can be achieved through the sole utilization of the RF section.

In case of an RF failure due to a miss classification from the neural-net, the final position estimate will be largely unaffected. This is due to the fact that Falcon is primarily reliant on VLP for localization. For example, consider a situation where the location reported by the FVLP system indicates that it is heading towards a region of uncertainty within the environment (row aligned lights in a hallway). At such a time, the system will start to add more weight to the RF measurement to ensure it correctly tracks through the region. The boundaries of the RF cells can be used as the regions of uncertainty. This means that once the system has a lock on where the target is, transient interference, even if it causes significant misclassification of cell position, does not significantly degrade the overall performance of the system.

In the extreme case where no luminaires are visible or the lights are turned off completely, the system can fall back to an RF based approach. This has no impact on the accuracy of the RF section.

In the worst case scenario where the lights are turned off and there is significant interference affecting wireless propagation, Falcon will fail to function. However, it should be noted that in these situations, standalone VLP or RF Localization systems would also fail.

VI. CONCLUSION & FUTURE WORKS

Falcon has shown that fusing a RF RSSI localization system with VLP can increase the robustness and performance in real life scenarios. In the hallway, a traditional trilateration based localization approach was impossible as the lights only provided information along one axis. By using the collocated RF resource to infer a region of interest, a horizontal displacement offset could be achieved. The VLP system used the displacement offset information provided as a secondary axis to attain sub decimeter level accuracy in that scenario. The wireless localization capability also keeps the system functional when the lights are off or there is occlusion.

The CNN for the RF data only focused on a stationary target at given locations. RSSI data for moving targets could be recorded and incorporated as a second channel to the CNN input image. The Falcon RF Classification stage uses the unique cell ID as the output. Sub cell RF localization could potentially be obtained by using the probabilities for each cell rather than the final cell id. By using the probabilities as weights, trilateration could be performed between the high probability cells to attain sub-cell resolution. Another option would be to explore different wireless localization approaches such as using SVM, particle filters or the Bayesian methodology.

A dynamic calibration scheme could be developed to check the accuracy of the RF classification vs the VLP, and to periodically retrain the CNN to ensure the accuracy remained acceptable.

The Falcon transmitter and receiver were kept in parallel. Receiver rotation due to the movement of the target would introduce error to the Lambertian model. Further development is required to measure the device rotation as it is being tracked and calibrate the model accordingly.

The experiments were conducted in the evening to avoid people walking through the target area. Therefore, the receiver did not need to mitigate the effect of ambient light as it was not strong enough to saturate the receiver. Further work will explore using variable gain amplifiers to allow the system to work under all lighting conditions.

REFERENCES

[1] M. Seifeldin, A. Saeed, A. E. Kosba, A. El-Keyi, and M. Youssef, "Nuzzer: A large-scale device-free passive localization system for wireless environments," *IEEE Trans. Mobile Comput.*, vol. 12, no. 7, pp. 1321–1334, Jul. 2013.

[2] *AS/NZS 1680.2.1:2008*. Accessed: Nov. 18, 2017. [Online]. Available: https://shop.standards.govt.nz/catalog/1680.2.1%3A2008%28AS%7CNZS%29/view

[3] X. Guo, S. Shao, N. Ansari, and A. Khreishah, "Indoor localization using visible light via fusion of multiple classifiers," *IEEE Photon. J.*, vol. 9, no. 6, Dec. 2017, Art. no. 7803716.

[4] P. H. Pathak, X. Feng, P. Hu, and P. Mohapatra, "Visible light communication, networking, and sensing: A survey, potential and challenges," *IEEE Commun. Surveys Tuts.*, vol. 17, no. 4, pp. 2047–2077, 4th Quart., 2015.

[5] D. Konings, B. Parr, C. Waddell, F. Alam, K. M. Arif, and E. M-K. Lai, "HVLP: Hybrid visible light positioning of a mobile robot," in *Proc. 24th Int. Conf. Mechatronics Mach. Vis. Pract. (M2VIP)*, 2017, pp. 1–6.

[6] G.-Y. Jin, X.-Y. Lu, and M.-S. Park, "An indoor localization mechanism using active RFID tag," in *Proc. IEEE Int. Conf. Sensor Netw., Ubiquitous, Trustworthy Comput. (SUTC)*, vol. 1, Jun. 2006, p. 4.

[7] D. Konings, A. Budel, F. Alam, and F. Noble, "Entity tracking within a Zigbee based smart home," in *Proc. 23rd Int. Conf. Mechatronics Mach. Vis. Pract. (M2VIP)*, 2016, pp. 1–6.

[8] M. Sugano, T. Kawazoe, Y. Ohta, and M. Murata, "Indoor localization system using RSSI measurement of wireless sensor network based on ZigBee standard," presented at the 6th, IASTED Int. Multi-Conf. Wireless Opt. Commun., Banff, Canada, 2006.

[9] C.-N. Huang and C.-T. Chan, "ZigBee-based indoor location system by k-nearest neighbor algorithm with weighted RSSI," *Procedia Comput. Sci.*, vol. 5, pp. 58–65, Jan. 2011.

[10] A. S. Paul and E. A. Wan, "RSSI-based indoor localization and tracking using sigma-point Kalman smoothers," *IEEE J. Sel. Topics Signal Process.*, vol. 3, no. 5, pp. 860–873, Oct. 2009.

[11] L. Zhao, H. Wang, P. Li, and J. Liu, "An improved WiFi indoor localization method combining channel state information and received signal strength," in *Proc. 36th Chin. Control Conf. (CCC)*, 2017, pp. 8964–8969.

[12] M. Altini, D. Brunelli, E. Farella, and L. Benini, "Bluetooth indoor localization with multiple neural networks," in *Proc. IEEE 5th Int. Symp. Wireless Pervasive Comput.*, May 2010, pp. 295–300.

[13] Y. Wang, Q. Ye, J. Cheng, and L. Wang, "RSSI-based Bluetooth indoor localization," in *Proc. 11th Int. Conf. Mobile Ad-Hoc Sensor Netw. (MSN)*, Dec. 2015, pp. 165–171.

[14] D. Konings, N. Faulkner, F. Alam, F. Noble, and E. Lai, "Do RSSI values reliably map to RSS in a localization system?" in *Proc. Workshop Recent Trends Telecommun. Res. (RTTR)*, Feb. 2017, pp. 1–5.

[15] S. Adler, S. Schmitt, and M. Kyas, "Path loss and multipath effects in a real world indoor localization scenario," in *Proc. 11th Workshop Positioning, Navigat. Commun. (WPNC)*, Mar. 2014, pp. 1–7.

[16] D. Konings, N. Faulkner, F. Alam, F. Noble, and E. M. K. Lai, "The effects of interference on the RSSI values of a ZigBee based indoor localization system," in *Proc. 24th Int. Conf. Mechatronics Mach. Vis. Pract. (M2VIP)*, 2017, pp. 1–5.

[17] Y.-S. Kuo, P. Pannuto, K.-J. Hsiao, and P. Dutta, "Luxapose: Indoor positioning with mobile phones and visible light," presented at the 20th Annu. Int. Conf. Mobile Comput. Netw. (MobiCom), Maui, HI, USA, 2014.

[18] L. Li, P. Hu, C. Peng, G. Shen, and F. Zhao, "Epsilon: A visible light based positioning system," in *Proc. NSDI*, 2014, pp. 331–343.

[19] J. Yang and Y. Chen, "Indoor localization using improved RSS-based lateration methods," in *Proc. IEEE Global Telecommun. Conf. (GLOBECOM)*, Nov. 2009, pp. 1–6.

[20] S. Mazuelas *et al.*, "Robust indoor positioning provided by real-time RSSI values in unmodified WLAN networks," *IEEE J. Sel. Topics Signal Process.*, vol. 3, no. 5, pp. 821–831, Oct. 2009.

[21] J. Xu, J. S. He, Y. Q. Zhang, F. Xu, and F. B. Cai, "A distance-based maximum likelihood estimation method for sensor localization in wireless sensor networks," *Int. J. Distrib. Sensor Netw.*, vol. 12, no. 4, Apr. 2016, Art. no. 2080536.

[22] J. So, J.-Y. Lee, C.-H. Yoon, and H. Park, "An improved location estimation method for WiFi fingerprint-based indoor localization," *Int. J. Softw. Eng. Appl.*, vol. 7, no. 3, pp. 77–86, May 2013.

[23] V. Honkavirta, T. Perala, S. Ali-Loytty, and R. Piche, "A comparative survey of WLAN location fingerprinting methods," in *Proc. 6th Workshop Positioning, Navigat. Commun.*, 2009, pp. 243–251.

[24] N. Pirzada, M. Y. Nayan, F. Subhan, M. F. Hassan, and M. A. Khan, "Comparative analysis of active and passive indoor localization systems," in *Proc. AASRI Conf. Parallel Distrib. Comput. Syst.*, vol. 5, Jan. 2013, pp. 92–97.

[25] W. Ruan, Q. Z. Sheng, L. Yao, T. Gu, M. Ruta, and L. Shangguan, "Device-free indoor localization and tracking through human-object interactions," in *Proc. IEEE 17th Int. Symp. World Wireless, Mobile Multimedia Netw. (WoWMoM)*, Jun. 2016, pp. 1–9.

[26] G. Deak, K. Curran, J. Condell, and D. Deak, "Detection of multi-occupancy using device-free passive localisation," *IET Wireless Sensor Syst.*, vol. 4, no. 3, pp. 130–137, Sep. 2014.

[27] S.-H. Fang and T.-N. Lin, "Indoor location system based on discriminant-adaptive neural network in IEEE 802.11 environments," *IEEE Trans. Neural Netw.*, vol. 19, no. 11, pp. 1973–1978, Nov. 2008.

[28] P. Cassarà, F. Potortì, P. Barsocchi, and M. Girolami, "Choosing an RSS device-free localization algorithm for ambient assisted living," in *Proc. Int. Conf. Indoor Positioning Indoor Navigat. (IPIN)*, 2015, pp. 1–8.

[29] H. Liu, H. Darabi, P. Banerjee, and J. Liu, "Survey of wireless indoor positioning techniques and systems," *IEEE Trans. Syst., Man, Cybern. C, Appl. Rev.*, vol. 37, no. 6, pp. 1067–1080, Nov. 2007.

[30] J. Drake, D. Najewicz, and W. Watts. General Electric Company. 2010. *Energy Efficiency Comparisons of Wireless Communication Technology Options for Smart Grid Enabled Devices*. [Online]. Available: https://energypriorities.com/library/ge_zigbee_vs_wifi_101209.pdf

[31] R. Challoo, A. Oladeinde, N. Yilmazer, S. Ozcelik, and L. Challoo, "An overview and assessment of wireless technologies and Co- existence of ZigBee, Bluetooth and Wi-Fi devices," *Procedia Comput. Sci.*, vol. 12, pp. 386–391, Nov. 2012.

[32] K. Shuaib, M. Boulmalf, F. Sallabi, and A. Lakas, "Co-existence of Zigbee and WLAN, a performance study," in *Proc. Wireless Telecommun. Symp.*, Apr. 2006, pp. 1–6.

[33] Z. Yang, Z. Zhou, and Y. Liu, "From RSSI to CSI: Indoor localization via channel response," *ACM Comput. Surv.*, vol. 46, no. 2, 2013, Art. no. 25.

[34] K. Wu, J. Xiao, Y. Yi, D. Chen, X. Luo, and L. M. Ni, "CSI-based indoor localization," *IEEE Trans. Parallel Distrib. Syst.*, vol. 24, no. 7, pp. 1300–1309, Jul. 2013.

[35] D. Halperin, W. Hu, A. Sheth, and D. Wetherall, "Tool release: Gathering 802.11n traces with channel state information," *ACM SIGCOMM Comput. Commun. Rev.*, vol. 41, no. 1, p. 53, Jan. 2011.

[36] Y. Xie, Z. Li, and M. Li, "Precise power delay profiling with commodity WiFi," presented at the 21st Annu. Int. Conf. Mobile Comput. Netw., Paris, France, 2015.

[37] S. Yiu, M. Dashti, H. Claussen, and F. Perez-Cruz, "Wireless RSSI fingerprinting localization," *Signal Process.*, vol. 131, pp. 235–244, Feb. 2017.

[38] Z. P. Li, M. Jiang, X. N. Zhang, X. Y. Chen, and W. K. Hou, "Space-time-multiplexed multi-image visible light positioning system exploiting pseudo-miller-coding for smart phones," *IEEE Trans. Wireless Commun.*, vol. 16, no. 12, pp. 8261–8274, Dec. 2017.

[39] L. Zeng *et al.*, "High data rate multiple input multiple output (MIMO) optical wireless communications using white led lighting," *IEEE J. Sel. Areas Commun.*, vol. 27, no. 9, pp. 1654–1662, Dec. 2009.

[40] Y. Cai, W. Guan, Y. Wu, C. Xie, Y. Chen, and L. Fang, "Indoor high precision three-dimensional positioning system based on visible light communication using particle swarm optimization," *IEEE Photon. J.*, vol. 9, no. 6, Dec. 2017, Art. no. 7908120.

[41] T. Q. Wang, Y. A. Sekercioglu, A. Neild, and J. Armstrong, "Position accuracy of time-of-arrival based ranging using visible light with application in indoor localization systems," *J. Lightw. Technol.*, vol. 31, no. 20, pp. 3302–3308, Oct. 15, 2013.

[42] T.-H. Do and M. Yoo, "TDOA-based indoor positioning using visible light," *Photon. Netw. Commun.*, vol. 27, no. 2, pp. 80–88, 2014.

[43] S.-Y. Jung, S. Hann, and C.-S. Park, "TDOA-based optical wireless indoor localization using LED ceiling lamps," *IEEE Trans. Consum. Electron.*, vol. 57, no. 4, pp. 1592–1597, Nov. 2011.

[44] G. B. Prince and T. D. C. Little, "A two phase hybrid RSS/AoA algorithm for indoor device localization using visible light," in *Proc. IEEE Global Commun. Conf. (GLOBECOM)*, Dec. 2012, pp. 3347–3352.

[45] Y. S. Eroglu, I. Guvenc, N. Pala, and M. Yuksel, "AOA-based localization and tracking in multi-element VLC systems," in *Proc. IEEE 16th Annu. Wireless Microw. Technol. Conf. (WAMICON)*, Apr. 2015, pp. 1–5.

[46] Z. Tian, K. Wright, and X. Zhou, "The darklight rises: Visible light communication in the dark: Demo," presented at the 22nd Annu. Int. Conf. Mobile Comput. Netw. (MobiCom), New York, NY, USA, 2016.
[47] X. Zhao and J. Lin, "Theoretical limits analysis of indoor positioning system using visible light and image sensor," *ETRI J.*, vol. 38, no. 3, pp. 560–567, 2016.
[48] K. Qiu, F. Zhang, and M. Liu, "Visible light communication-based indoor localization using Gaussian process," in *Proc. IEEE/RSJ Int. Conf. Intell. Robots Syst. (IROS)*, Sep. 2015, pp. 3125–3130.
[49] K. Moriya, M. Fujimoto, Y. Arakawa, and K. Yasumoto, "Indoor localization based on distance-illuminance model and active control of lighting devices," in *Proc. Int. Conf. Indoor Positioning Indoor Navigat. (IPIN)*, 2016, pp. 1–6.
[50] H. Zou, Z. Chen, H. Jiang, L. Xie, and C. Spanos, "Accurate indoor localization and tracking using mobile phone inertial sensors, WiFi and iBeacon," in *Proc. IEEE Int. Symp. Inertial Sensors Syst. (INERTIAL)*, Mar. 2017, pp. 1–4.
[51] Y. Li, J. Chen, Y. Shi, Y. Cheng, and L. Wang, "WiFi-assisted multi-floor indoor localization with inertial sensors," in *Proc. 8th Int. Conf. Wireless Commun. Signal Process. (WCSP)*, 2016, pp. 1–5.
[52] J. L. Carrera, Z. Zhao, T. Braun, and Z. Li, "A real-time indoor tracking system by fusing inertial sensor, radio signal and floor plan," in *Proc. Int. Conf. Indoor Positioning Indoor Navigat. (IPIN)*, 2016, pp. 1–8.
[53] L. Buonocore, S. R. B. dos Santos, A. A. Neto, and C. L. Nascimento, "FastSLAM filter implementation for indoor autonomous robot," in *Proc. IEEE Intell. Vehicles Symp. (IV)*, Jun. 2016, pp. 484–489.
[54] B. Vincke, A. Elouardi, and A. Lambert, "Real time simultaneous localization and mapping: Towards low-cost multiprocessor embedded systems," *EURASIP J. Embedded Syst.*, vol. 2012, no. 1, p. 5, Dec. 2012.
[55] J. Vazquez and C. Malcolm, "Fusion of triangulated sonar plus infrared sensing for localization and mapping," in *Proc. Int. Conf. Control Automat.*, vol. 2, 2005, pp. 1097–1102.
[56] J. Schmidhuber, "Deep learning in neural networks: An overview," *Neural Netw.*, vol. 61, pp. 85–117, Jan. 2015.
[57] D. Han, S.-H. Jung, and S. Lee, "A sensor fusion method for Wi-Fi-based indoor positioning," *ICT Express*, vol. 2, no. 2, pp. 71–74, Jun. 2016.
[58] Z. Yang, C. Wu, and Y. Liu, "Locating in fingerprint space: Wireless indoor localization with little human intervention," presented at the 18th Annu. Int. Conf. Mobile Comput. Netw., Istanbul, Turkey, 2012.
[59] Y. Wang and X. Xu, "Indoor localization service based on the data fusion of Wi-Fi and RFID," in *Proc. IEEE Int. Conf. Web Services (ICWS)*, Jun. 2016, pp. 180–187.
[60] R. Zhang, W.-D. Zhong, D. Wu, and K. Qian, "A novel sensor fusion based indoor visible light positioning system," in *Proc. IEEE Globecom Workshops (GC Wkshps)*, Dec. 2016, pp. 1–6.
[61] B. Xie *et al.*, "LIPS: A light intensity–based positioning system for indoor environments," *ACM Trans. Sensor Netw.*, vol. 12, no. 4, 2016, Art. no. 28.
[62] M. Yasir, S.-W. Ho, and B. N. Vellambi, "Indoor positioning system using visible light and accelerometer," *J. Lightw. Technol.*, vol. 32, no. 19, pp. 3306–3316, Oct. 1, 2014.
[63] S. H. Yang, H. S. Kim, Y. H. Son, and S. K. Han, "Three-dimensional visible light indoor localization using AOA and RSS with multiple optical receivers," *J. Lightw. Technol.*, vol. 32, no. 14, pp. 2480–2485, Jul. 15, 2014.
[64] J. M. Kahn and J. R. Barry, "Wireless infrared communications," *Proc. IEEE*, vol. 85, no. 2, pp. 265–298, Feb. 1997.
[65] B. Lehman and A. J. Wilkins, "Designing to mitigate effects of flicker in LED lighting: Reducing risks to health and safety," *IEEE Power Electron. Mag.*, vol. 1, no. 3, pp. 18–26, Sep. 2014.
[66] S. He and S.-H. G. Chan, "Wi-Fi fingerprint-based indoor positioning: Recent advances and comparisons," *IEEE Commun. Surveys Tuts.*, vol. 18, no. 1, pp. 466–490, Jan. 2015.
[67] J. Borenstein and Y. Koren, "Real-time obstacle avoidance for fast mobile robots," *IEEE Trans. Syst., Man, Cybern.*, vol. 19, no. 5, pp. 1179–1187, Sep./Oct. 1989.
[68] J. Barraquand, B. Langlois, and J.-C. Latombe, "Numerical potential field techniques for robot path planning," *IEEE Trans. Syst., Man, Cybern.*, vol. 22, no. 2, pp. 224–241, Mar./Apr. 1992.
[69] D. L. Hall and A. Steinberg, *Dirty Secrets in Multisensor Data Fusion*. State College, PA, USA: Pennsylvania State Univ. Park Applied Research Lab, 2001.

DANIEL KONINGS (M'17) received the B.E. degree (Hons.) in computer systems and electronics engineering from Massey University, Auckland, New Zealand, in 2014, where he is currently pursuing the Ph.D. degree with the School of Engineering and Advanced Technology. His research interests include indoor localization, digital signal processing, machine learning, IoT, and wireless sensor networks.

BADEN PARR received the B.E. degree (Hons.) in Computer Systems and Electronics Engineering from Massey University, Auckland, New Zealand, in 2017, where he is currently pursuing the Ph.D. degree with the School of Engineering and Advanced Technology. His research interests include visible light communication, drone research, machine learning, IoT, and wireless sensor networks.

FAKHRUL ALAM (M'17) received the B.Sc. degree (Hons.) in electrical and electronic engineering from BUET, Bangladesh, and the M.S. and Ph.D. degrees in electrical engineering from Virginia Tech, USA. He is currently a Senior Lecturer with the School of Engineering and Advanced Technology, Massey University, New Zealand. His research interests include indoor localization, 5G and visible light communication, disaster management with 5G, IoT, and wireless sensor networks. He is a member of the Institution of Engineering and Technology.

EDMUND M.-K. LAI (M'82–SM'96) received the B.E. degree (Hons.) and the Ph.D. in electrical engineering degree from The University of Western Australia in 1982 and 1991, respectively. He has held faculty positions at universities in Australia, Hong Kong, and Singapore. He is currently a Professor of information engineering with the Auckland University of Technology, New Zealand. His research interests include digital signal processing, digital communications and networks, computational and swarm intelligence, and artificial neural networks. He is a fellow of the Institution of Engineering and Technology.